Value $K = 1.44$ is approximately two times smaller than in Table 6-3.

(e) Drop surface.

Specific drop surface A_D follows from Eq. (3-70):

$$A_D = \frac{6}{D_{32}} = \frac{6}{0.00592} = 1010 \text{ cm}^2/\text{cm}^3$$

The drop surface equals

$$A = A_D V_w = 1010 \times 0.304 = 307 \text{ cm}^2/\text{cycle}$$

5-2 DESIGN OF A SWIRL ATOMIZER

There is an extensive literature devoted to calculation methods for swirl atomizers, especially simplex atomizers. There are two main approaches to the calculations. The first uses the so-called principle of the maximum flow, the second the equation of conservation of momentum. The first approach is historically older and more popular than the second. Both approaches differ with respect to the methodology used, but they consider the establishment of relationships between the same characteristic dimensions of an atomizer, such as d_0, A_p, R, i.e., geometric constant K, as well as spray parameters μ, ϵ, α.

A literature survey and a comparison of results obtained by different calculation methods are presented in [15]. The comparison shows that some discrepancies do exist; however, they are of less importance when it comes to the design of the atomizers for practical applications. In such cases, simplicity of the calculation method is most important.

Newer work on the design of swirl atomizers has appeared, including [4, 16, 17]. Methods based on the Navier-Stokes equations are considered critically in [6]; however, new work on this subject was published more recently [14]. A calculation method based on the principle of maximum flow with the modified free vortex equation is presented in [18, 19] and a method based on the principle of conservation of momentum in [13].

Special attention must be paid to [20, 21]. The analysis is based on the theoretically calculated liquid film thickness in the discharge orifice. This thickness was related to spray angle α and to the value of the conventional velocity coefficient K_v. Knowledge of this coefficient and its changes caused by the atomizer dimensions, liquid properties, and atomization conditions is the basic condition that allows the design of an atomizer.

5-2.1 Simplex Atomizers

Ideal liquid theory [15]. A model of the design a simplex atomizer is presented in Fig. 5-9. The liquid is fed through tangential orifice 1 with diameter d_p and cross-sectional area A_p to swirl chamber 2 with diameter $D_s = 2R + d_p$, and

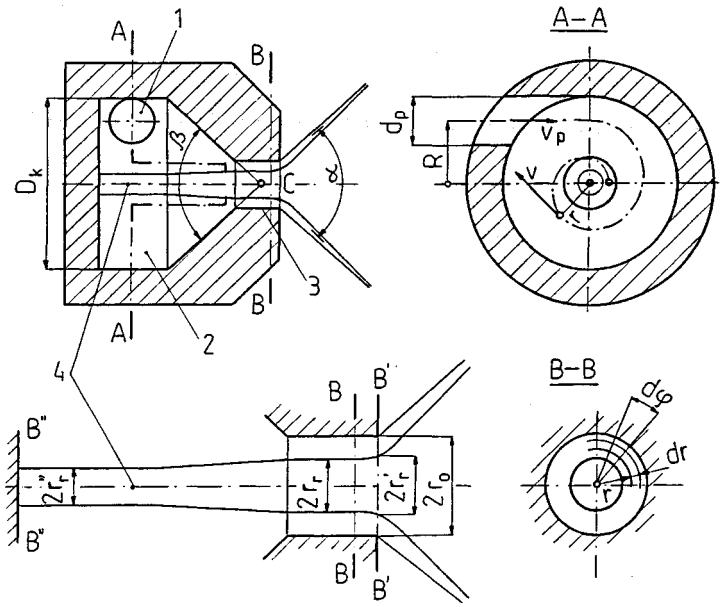

Figure 5-9 Design model for a simplex swirl atomizer. 1, Inlet orifice; 2, swirl chamber; 3, discharge orifice; 4, gas core.

the inlet of the tangential orifice is located on radius R. In general, there are several inlet orifices and in this case

$$iA_p = i\pi r_p^2 = i\frac{\pi d_p^2}{4} \tag{5-43}$$

where i is the number of orifices. Tangential orifices often have a shape other than circular, which does not affect the calculation methodology. The liquid discharges from outlet orifice 3 with diameter $d_0 = 2r_0$.

The motion of the liquid inside the atomizer is complex. In the region of the swirl chamber this motion consists of a potential vortex and the motion caused by the negative source whose position coincides with vertex C of the transient cone. In the region of the cylindrical discharge orifice the motion consists of a potential vortex and an axial motion. All velocity components should be considered, i.e. axial u, circumferential v, and radial w; the last one is significantly lower than the others.

The liquid discharges not through the whole cross section but through an annular one. The central part of the cross section is filled by *gas core* 4, which in Fig. 5-9 is shown in a smaller and larger scale. The area of annular cross section A is

$$A = \pi(r_0^2 - r_r^2) = \epsilon\pi r_0^2 \tag{5-44}$$

hence the efficiency of filling of the discharge orifice ϵ has the following form:

$$\epsilon = \frac{A}{A_0} = \frac{\pi(r_0^2 - r_2^2)}{\pi r_0^2} = 1 - \left(\frac{r_r}{r_0}\right)^2 \tag{5-45}$$

where $A_0 = \pi r_0^2 = \pi d_0^2/4$ is the area of the discharge orifice and r_r is the gas core diameter.

Circumferential velocity component V changes according to the principle of the potential vortex, which is represented by the equation

$$vr = \text{const} \tag{5-46}$$

A free vortex has a singular point at $r = 0$, for which $V = +\infty$ and pressure $P = -\infty$. If so, a free vortex can exist only in the region with radius $r \geq r_r$. The circumferential velocity increases at the core boundary to a certain maximum value v_{max}.

Axial velocity u occurs inside the swirl chamber at a radius slightly larger than radius r_0.

This velocity causes the circumferential velocity v to decrease and therefore velocity v_{max} is lower, as would follow from the free vortex equation. This fact will not, however, be incorporated in the analysis.

In the region of the gas core $r < r_r$, a so-called *rigid vortex* exists in which the gas originating from the atomizer's ambient rotates as a rigid body with constant angular velocity

$$\omega = \frac{v}{r} = \frac{v_{max}}{r_r} = \text{const} \tag{5-47}$$

Velocity v_{max} can be calculated from the Bernoulli equation (for $w = 0$)

$$\frac{\rho}{2}(u^2 + v^2) + P = P_t = \text{const} \tag{5-48}$$

if the values u and P are known at the core boundary. The pressure is equal to $P \approx P_0$, where P_0 is the ambient pressure. Axial velocity u varies and is constant only in the region of the outlet orifice. Pressure P_t is the total liquid pressure. According to the equation of conservation of angular momentum with respect to the chamber axis, we can write

$$v_p R = vr = v_{max} r_r = \text{const} \tag{5-49}$$

The following assumptions will be made for further considerations:

The liquid is ideal.
The velocity field is a potential one in the whole region between the chamber walls and the gas core.
Angular momentum, according to Eq. (5-49), is constant.
There is no gravity.
The flow is stable and axisymmetric.
There is no radial component of velocity ($w = 0$).

According to Fig. 5-9, a liquid element on radius r, with width dr, length $r\,d\varphi$, and unit thickness is acted on by a pressure force and mass force. The condition of equilibrium of these forces has the form

$$r\,d\varphi\,dP = \frac{v^2}{r}\,dm \tag{5-50}$$

Substituting element of mass $dm = \varphi r\,d\varphi$ and velocity v from Eq. (5-49),

$$v = \frac{v_{\max} r_r}{r} \tag{5-51}$$

into Eq. (5-50), one obtains

$$dP = \rho v_{\max}^2 r_r^2 \frac{dr}{r^3} \tag{5-52}$$

After integration Eq. (5-52) assumes the following form:

$$P = -\frac{\rho}{2} v_{\max}^2 r_r^2 \frac{1}{r^2} + C \tag{5-53}$$

Constant C follows from the condition that on the gas core boundary, i.e., for $r = r_r$, the overpressure equals zero, hence

$$C = \frac{\rho}{2} v_{\max}^2$$

By substituting C and $v_{\max}$ from Eq. (5-51) into (5-53) we obtain the equation of the pressure distribution in the transverse cross section of the discharge orifice:

$$P = \frac{\rho}{2}(v_{\max}^2 - v^2) \tag{5-54}$$

Substituting pressure P from Eq. (5-54) into Eq. (5-48) one obtains

$$u = \sqrt{\frac{2P_t}{\rho} - v_{\max}^2} = \text{const} \tag{5-55}$$

As seen, axial velocity component u is uniform in the transverse cross section of the discharge orifice, since in the given conditions $P_t = \text{const}$ and $v_{\max} = \text{const}$. This uniformity of velocity u is, however, disturbed between cross sections B–B and B'–B'. This is caused by the fact that between these cross sections the static centrifugal overpressure is transformed into the dynamic pressure, since in cross section B'–B' pressure should be constant and equal to the ambient pressure. Therefore velocity u is higher at the wall than at the core boundary. The change of velocity u was not accounted for in Fig. 3-12.

Distribution of axial velocity w in cross section B'–B' can be determined as follows, Velocity v_p from Eq. (5-60) and Q from Eq. (5-62) should be substituted into Eq. (5-49), and after taking into account K from Eq. (4-1) we obtain

$$v = \frac{\mu K r_0}{r} \sqrt{\frac{2P_t}{\rho}} \tag{5-56}$$

Velocity v should be introduced into Eq. (5-48), assuming that overpressure $P = 0$ in cross section B'–B'. Hence

$$u = \sqrt{1 - \frac{\mu^2 K^2 r_0^2}{r^2}} \sqrt{\frac{2P_t}{\rho}} \tag{5-57}$$

Equation (5-57) expresses the distribution of axial velocity component W in the discharging cross section, i.e., in the cross section B'–B'. It follows from this equation that velocity u increases as radius r increases.

Radius r_r of the gas core changes along the chamber axis in a following way. The smaller the axial velocity component, the higher (according to the Bernoulli equation) the circumferential component. Its increase causes a decrease of radius r_r. The smaller radius r_r'' occurs on the back wall of the swirl chamber (Fig. 5-9), where the axial velocity has its minimum value; the largest radius r_r' occurs on the front wall, where the axial velocity has its maximum value.

Radius r_r' of the gas core can be calculated from the following integral equation using Eq. (5-62):

$$Q = \int_{r_r'}^{r_0} 2\pi r\, dr\, u = \mu \pi r_0^2 \sqrt{\frac{2P_t}{\rho}}$$

Substituting velocity u from Eq. (5-57), we obtain the following equation:

$$\mu = \sqrt{1 - \mu^2 K^2} - S\sqrt{S^2 - \mu^2 K^2} - \mu^2 K^2 \ln \frac{1 + \sqrt{1 - \mu^2 K^2}}{S + \sqrt{S^2 - \mu^2 K^2}} \tag{5-58}$$

where $S = r_r'/r_0$ is a dimensionless radius of the gas core in the discharge cross section.

Solving Eq. (5-58) graphically with respect to S, we must assign to each value of K a corresponding value of μ from Fig. 5-11. The solution is shown in Fig. 5-10 as curve 1. In addition, the changes of the dimensionless core r_r/r_0 and r_r''/r_0 (curves 2 and 3) are shown. Curve 1 assumes the highest position since it refers to the larger radius r_r'. The largest differences in the curve positions correspond to small values of constant K.

Volumetric flow rate Q determined by using Eq. (5-44) equals

$$Q = Au = \epsilon \pi r_0^2 u \tag{5-59}$$

On the other hand, the same flow rate can be determined at the inlet to the swirl chamber by using Eq. (5-43):

$$Q = iA_p v_p = i\pi r_p^2 v_p \tag{5-60}$$

Substituting velocity $v_{\max}$ from Eq. (5-49) and velocity v_p from Eq. (5-60) into Eq. (5-55), we obtain

$$u = \sqrt{\frac{2P_t}{\rho} - \frac{R^2 Q^2}{i^2 \pi^2 v_p^2 r_r^2}} \tag{5-61}$$

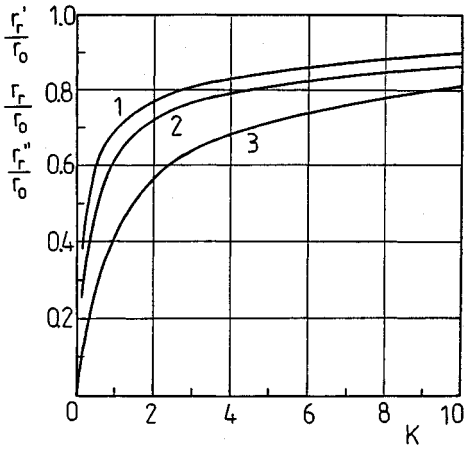

Figure 5-10 Dimensionless radii of the gas core. 1, On the outlet from atomizer r_r'/r_0; 2, inside the outlet orifice r_r/r_0; 3, on the back wall of swirl chamber r_r''/r_0.

Comparing this velocity u with velocity u obtained from Eq. (5-59) and taking into account Eq. (5-45) and geometric constant K from Eq. (4-1), we obtain volumetric liquid flow rate Q:

$$Q = \frac{1}{\sqrt{K^2/(1-\epsilon) + 1/\epsilon^2}} \pi r_0^2 \sqrt{\frac{2P_t}{\rho}} = \mu A_0 \sqrt{\frac{2\Delta P}{\rho}} \tag{5-62}$$

or mass liquid flow rate G

$$G = \rho Q = \mu A_0 \sqrt{2\rho \Delta P} \tag{5-63}$$

Equations (5-62) and (5-63) are identical in notation to Eq. (3-3) and (3-4), since the drop of static pressure ΔP in the atomizer is approximately equal to liquid overpressure P_t with respect to ambient pressure P_0, i.e., $\Delta P \approx P_t$. Discharge coefficient μ of a simplex swirl atomizer is therefore equal to

$$\mu = \frac{1}{\sqrt{K^2/(1-\epsilon) + 1/\epsilon^2}} \tag{5-64}$$

As seen, discharge coefficient μ depends on two quantities: the geometric constant K and the efficiency of filling the discharge orifice ϵ.

Discharge coefficient μ is a complex function of ϵ, since it has small values for both small and large filling efficiency ϵ, passing through a maximum. The explanation is as follows. Small efficiency of filling ϵ corresponds to a large diameter of the gas core, i.e., to a small equivalent flow cross section, and large efficiency of filling ϵ means a small diameter of the gas core and therefore high circumferential velocity v and small axial velocity u.

At the outlet of the atomizer the gas core establishes an efficiency of filling ϵ, that ensures the maximum value of the discharge coefficient μ, i.e., the maximum liquid flow for a given pressure drop. This is the *principle of maximum*

flow. The first author who implemented this principle for swirl atomizers was Abramovich [3]. Only when this principle is satisfied do the conditions of stable flow exist.

Flow in a swirl atomizer has a free liquid surface at the boundary of the gas core and in this respect is similar to the flow in an open channel. The maximum flow principle in a swirl atomizer is equivalent to the principle of the maximum (critical) flow in an open channel; the difference is that in open channels a free surface develops because of gravity forces and in the case of a swirl atomizer because of centrifugal force.

A stable flow occurs when the flow velocity is equal to the velocity of wave propagation on the free liquid surface, in this case on the surface of the gas core. In [3] an equation was derived for the velocity of propagation of waves in a swirl atomizer and it was demonstrated that this velocity is equal to the axial velocity during the maximum flow. However, it follows from experiments [17] that on the vortex surface a transition can occur from supercritical flow (Fr $<$ 1) to subcritical flow (Fr $>$ 1), where Fr is the Froude number. The liquid energy reaches its maximum when the Froude number is equal to unity (Fr = 1).

Efficiency of filling ϵ ensures the maximum value of discharge coefficient μ when

$$\frac{d\mu}{d\epsilon} = 0$$

Differentialtion of Eq. (5-64) gives

$$K = \frac{(1 - \epsilon)\sqrt{2}}{\epsilon\sqrt{\epsilon}} \tag{5-65}$$

From Eqs. (5-64) and (5-65) we have the following expression for the discharge coefficient:

$$\mu = \epsilon\sqrt{\frac{\epsilon}{2 - \epsilon}} \tag{5-66}$$

Figure 5-11 presents function $\epsilon = f(K)$ from Eq. (5-65) and function $\mu = f(K)$ from Eqs. (5-65) and (5-66).

The *spray angle* follows from the ratio of the circumferential and axial velocities (Sec. 3-2.1). Drops circumscribe a hyperboloidal surface of revolution whose asymptote is a conical surface. Angle α can be calculated in a simplified way from the ratio

$$\operatorname{tg}\frac{\alpha}{2} = \frac{\hat{v}}{u} \tag{5-67}$$

where v is the circumferential velocity component on a mean radius r (Fig. 5-12)

$$\hat{r} = \tfrac{1}{2}(r_0 + r_r) \tag{5-68}$$

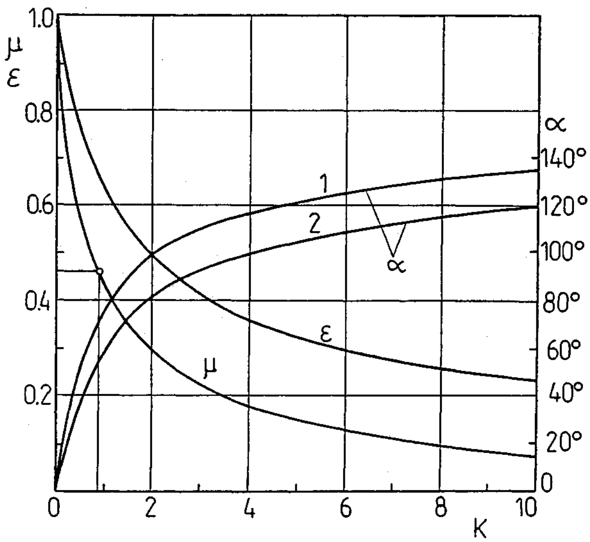

Figure 5-11 Dependence of the discharge coefficient μ, inlet orifice filling efficiency ϵ, and spray angle α on geometric constant of a swirl atomizer K. 1, According to Eq. (5-72); 2, according to Eq. (5-75).

Formula (5-67) differs from formula (3-27) in that in the first case $\hat{v}$ is the circumferential velocity on mean radius r and in the second case v_m is the arithmetic mean of the circumferential components or radii r_0 and r_r. The difference is caused by the fact that the distribution of circumferential component v is not linear but hyperbolic [Eq. (5-49)]. In both cases the same simplification was adopted, namely u = const in the discharge cross section.

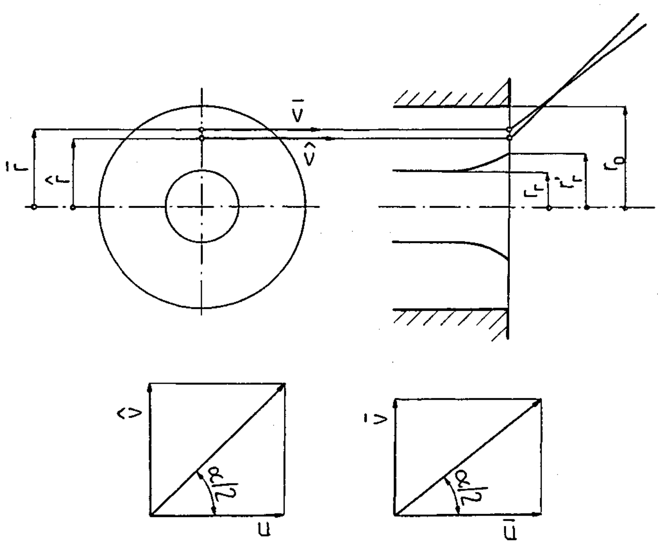

Figure 5-12 Scheme for calculating angle α using Eqs. (5-67) and (5-73).

Circumferential velocity v on the radius $\hat{r}$ can be calculated from the free vortex equation

$$\hat{v}\hat{r} = v_p R \tag{5-69}$$

Taking into account Eq. (5-68), we obtain

$$\hat{v} = \frac{v_p R}{\frac{1}{2}(r_0 + r_r)} \tag{5-70}$$

Axial velocity u can be derived from Eqs. (5-59) and (5-60):

$$u = \frac{v_p r_p^2}{\epsilon r_0^2} \tag{5-71}$$

For simplicity it was assumed that $i = 1$, i.e., one tangential inlet orifice, which does not change the methodology of calculations.

Substituting $\hat{v}$ and u from Eqs. (5-70) and (5-71) into Eq. (5-67) and taking into account

$$K = \frac{Rr_0}{r_p^2}$$

and ϵ from Eq. (5-45) and K from Eq. (5-65), we obtain finally

$$\operatorname{tg}\frac{\alpha}{2} = \frac{2\sqrt{2}(1-\epsilon)}{\sqrt{\epsilon}(1+\sqrt{1-\epsilon})} \tag{5-72}$$

This equation is exceptionally simple because it relates angle α only to the efficiency of filling ϵ. Due to the simplifying assumption (u = const), angle α is too large (Fig. 5-11).

For a more precise calculation one should use the following relationship:

$$\operatorname{tg}\frac{\alpha}{2} = \frac{\bar{v}}{\bar{u}} \tag{5-73}$$

where $\bar{v}$ and $\bar{u}$ are velocity components on the mean radius $\bar{r}$ (Fig. 5-12)

$$\bar{r} = \frac{1}{2}(r_0 + r_r') = \frac{r_0}{2}(1+S) \tag{5-74}$$

Substituting $r = \bar{r}$ into Eqs. (5-56) and (5-57), we obtain

$$\bar{v} = \frac{2\mu K}{1+S}\sqrt{\frac{2P_t}{\rho}}$$

and therefore

$$\bar{u} = \sqrt{1 - \frac{4\mu^2 K^2}{(1+S)^2}}\sqrt{\frac{2P_t}{\rho}}$$

$$\operatorname{tg}\frac{\alpha}{2} = \frac{\bar{v}}{\bar{u}} = \frac{2\mu K}{\sqrt{(1+S)^2 - 4\mu^2 K^2}} \tag{5-75}$$

Figure 5-11 shows angle α derived from Eq. (5-75). For $k = 0$, $\alpha = 0$ and for $K \to \infty$, α tends to 180°. Condition $K = 0$ corresponds to the vortex-free flow that is typical of jet atomizers.

Viscous liquid theory [15]. The effect of viscosity on the operation of a swirl atomizer has been discussed in numerous publications but there are still some controversies. Due to viscosity, friction forces develop at the wall of the swirl chamber which cause the angular momentum to decrease. As a result, the angular momentum in the discharge orifice should be smaller than at the inlet to the swirl chamber, and therefore the radius of the gas core and angle α should decrease and the discharge coefficient μ should increase. Therefore an unexpected situation occurs when the discharge coefficient of a viscous liquid is larger than that of an ideal liquid.

The motion of the viscous liquid was considered in [3] based on the condition of equilibrium of forces acting on a liquid element. As a result, the following approximate value of the flow ratio was obtained:

$$\mu = \frac{1}{\sqrt{K_\lambda^2/(1-\epsilon) + 1/\epsilon^2}} \tag{5-76}$$

As seen, Eq. (5-76) differs from Eq. (5-64) in the sense that constant K is replaced by K_λ. Equivalent geometric constant K_λ is given by

$$K_\lambda = \frac{K}{1 + (\lambda/2)(B^2/i - K)} \tag{5-77}$$

where

$$B = \frac{R}{r_p} \quad \text{or} \quad B = R\sqrt{\frac{\pi}{A_p}} \tag{5-78}$$

Here λ is a friction coefficient and parameters i, R, r_p, A_p follow from Fig. 5-9.

One can use curve $\mu = f(K)$ from Fig. 5-11, but value K_λ instead of K should be used as the abscissa. Since $K_\lambda < K$, coefficient μ is larger than that for an ideal liquid.

For a viscous liquid Eq. (5-65) has the same form, namely

$$K_\lambda = \frac{(1-\epsilon)\sqrt{2}}{\epsilon\sqrt{\epsilon}} \tag{5-79}$$

It follows from the condition $K_\lambda < K$ (Fig. 5-11) that for a viscous liquid the efficiency of filling ϵ is higher and the radius of the gas core r_r is smaller than for an ideal liquid. The spray angle can be expressed approximately by an equation similar to Eq. (5-75), namely

$$\operatorname{tg}\frac{\alpha}{2} = \frac{2\mu K_\lambda}{\sqrt{(1+S)^2 - 4\mu^2 K^2}} \tag{5-80}$$

Since $K_\lambda < K$, from Fig. 5-11 we obtain a smaller value of angle α than for an ideal liquid.

Substituting K and B to Eq. (5-77), we obtain

$$K_\lambda = \frac{Rr_0}{ir_p^2 + (\lambda/2)R(R - r_0)} \tag{5-81}$$

Two cases will be considered: changes of R and r_p for other parameters held constant. When $R \to \infty$ then for the ideal liquid $K \to \infty$, i.e., $\mu \to 0$ and $\alpha \to 180°$; for a viscous liquid from Eq. (5-81) it follows that K_λ increases to a certain maximum and subsequently decreases to zero. When $r_p \to 0$, then for the ideal liquid $K \to \infty$, but for a viscous liquid it follows from Eq. (5-81) that K_λ increases to a certain finite value.

It is seen therefore that the maximum value K_λ depends on how geometric constant K increases, whether it is due to the increase of R or the decrease of r_p. A "viscosity barrier" of some kind develops, which is manifested by the fact that equivalent geometric constant K_λ reaches a maximum to which minimum value $\mu_{\min}$ and maximum value $\alpha_{\max}$ correspond.

As opposed to the theoretical consideration of the effect of viscosity, there are many works in which the viscosity is taken into account empirically. This will be discussed in Sec. 6-2.

Design method [15]. The aim of the design is to determine the dimensions of a simplex swirl atomizer for the following data: Q or G, α, ΔP, ρ, and ν. First one calculates the basic dimensions incorporated in geometric constant K and then the other dimensions (Fig. 5-13). As it turns out, it is not a unique problem. The ambiguity is caused by the fact that the same value of constant K can be derived from an appropriate selection of various values R, i, d_p, d_0. That is why one should follow some recommendations dictated by experience gathered up until now.

The *first phase of calculations* refers to an ideal liquid. For given angle α from Fig. 5-11 (curve 2) we determine geometric constant K and subsequently discharge coefficient μ. From Eq. (5-63) we calculate the discharge orifice diameter

$$d_0 = \sqrt{\frac{4G}{\pi\mu\sqrt{2\rho P_t}}} \tag{5-82}$$

The geometric constant contains now three unknown quantities, R, i, d_p

$$K = \frac{2Rd_0}{id_p^2} \tag{5-83}$$

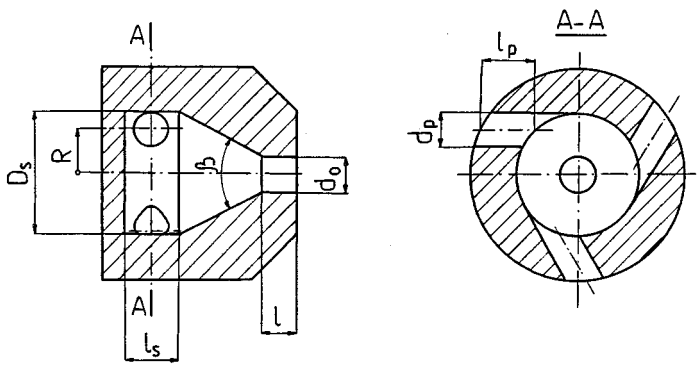

Figure 5-13 Basic dimensions of a simplex swirl atomizer.

two of which have to be assumed. It is most convenient to assume the number of orifices and radius of swirling. Most commonly, $i = 2$ to 4 and $R = (2–5)r_0$ are used. In some instances the dimensions of the atomizer dictate the value of R. From Eq. (5-83) we calculate the diameter of the tangential inlet orifices.

$$d_p = \sqrt{\frac{2Rd_0}{iK}} \tag{5-84}$$

In the case of orifices with a shape other than circular, instead of d_p we determine A_p from Eq. (4-1).

The *second phase of calculations* refers to the assessment of the viscosity effect. The Reynolds number at the inlet to the atomizers is

$$\mathrm{Re} = \frac{v_p d}{\nu} \tag{5-85}$$

where d is the diameter of the equivalent orifice, which can be determined as follows

$$\frac{\pi d^2}{4} = i\frac{\pi d_p^2}{4}$$

hence

$$d = \sqrt{i}\, d_p$$

Velocity v_p is given by

$$v_p = \frac{4G}{\rho i \pi d_p^2}$$

Substituting it to Eq. (5-85), we obtain

$$\mathrm{Re} = \frac{4G}{\pi\rho\nu\sqrt{i}\, d_p} \tag{5-86}$$

Friction coefficient λ follows from the formula

$$\lg \lambda = \frac{25.8}{(\lg \mathrm{Re})^{2.58}} - 2 \tag{5-87}$$

Equation (5-87) has been established as a result of extensive investigations of atomizers in the range $\mathrm{Re} = 10^3$–10^5. Values λ determined from Eq. (5-87) are significantly larger than would follow from well-known equations used in hydraulics. This is due to by high transverse gradients of pressure in the wall boundary.

The effect of liquid viscosity can be neglected when the following inequality is satisfied:

$$\frac{B^2}{i} - K \leq \frac{2}{\lambda}(\Phi^{1.5} - 1) \tag{5-88}$$

where Φ denotes ratio of discharge coefficients μ for a viscous and an ideal liquid.

Considering the selection of the value of radius R, remember that R should be small and simultaneously the area of the inlet orifices should be small in order to overcome the viscosity barrier. The higher K is, i.e., the larger angle α is required, the smaller radius R should be. Also, the smaller the flow rate and the higher the liquid viscosity, the smaller radius R should be. For liquids with moderate viscosity we should assume

$$B = \frac{R}{r_p} < 4\text{–}5$$

which follows from the fact that the following condition should be satisfied:

$$\frac{B^2}{i} - K < 5\text{–}10$$

One should not, however, assume too small values of B and R, since this would cause the atomizer's dimensions to be too small.

In tangential inlet orifices, liquid counteraction occurs and therefore the actual area of cross section A' of each inlet orifice should be increased in such a way that the jet has cross section area A_p. From the definition of the *contraction coefficient* [Eq. (5-3)] follows

$$\varphi = \frac{A_p}{A'_p} = \left(\frac{d_p}{d'_p}\right)^2$$

hence

$$d'_p = \frac{d_p}{\sqrt{\varphi}} \tag{5-89}$$

The contraction coefficient is assumed to be $\varphi = 0.85$–0.90.

The *third phase of calculations* concerns the determination of the remaining dimensions of the atomizer (Fig. 5-13). The following recommendations are of a general character; the more detailed recommendations will be given in Sec. 6-2.

The diameter of the swirl chamber D_s is

$$D_s = 2R + d'_p$$

The length of the swirl chamber l_s should be slightly larger than that of the inlet orifice. It suffices for a liquid to make one fourth to one third of rotations, since a long chamber determines the atomization conditions.

The inlet orifices should have the proper length l_s so that jets entering the swirl chamber are not deflected from the tangential direction. We recommend $l_s = (1.5\text{–}3.0)d'_p$.

The discharge orifice should not be too long in order not to decrease angle α. For $K_\lambda < 4\text{–}5$ we recommend $l = (0.5\text{–}1.0)d_0$; for $K_\lambda > 4\text{–}5, l = (0.25\text{–}0.5)d_0$. The angle of the transient cone most commonly equals $\beta = 60\text{–}120°$; smaller angles β cause an increase of the discharge coefficient μ and decrease of angle α.

The calculation method presented refers not only to atomizers with tangential orifices but also to atomizers with a swirling insert. In the latter case the radius of swirling R is equal to the radius of the swirling grooves. Geometric constant K follows from Eq. (4-1), where A_p is a cross section of an individual groove and i is the number of grooves.

Example 5-2 Design an atomizer of a gas turbine according to Fig. 5-13 for the following data [3]:

$G = 144$ kg/h $= 0.04$ kg/s is the flow rate of kerosene
$\alpha = 60°$ is the spray angle
$P_t = \Delta P = 3.45$ MPa is the pressure drop
$\rho = 830$ kg/m^3 is the density of kerosene
$\nu = 2.2 \times 10^{-6}$ m^2/s is the kinematic viscosity of kerosene

SOLUTION For angle $\alpha = 60°$ from Fig. 5-11 we obtain

$$K \approx 0.9, \qquad \mu \approx 0.46$$

From Eq. (5-82)

$$d_0 = \sqrt{\frac{4G}{\pi\mu\sqrt{2\rho\,\Delta P}}} = \sqrt{\frac{4 \times 0.04}{\pi \times 0.46\sqrt{2 \times 830 \times 3.45 \times 10^6}}}$$

$$\approx 0.0012 \text{ m} = 1.2 \text{ mm}$$

It was assumed that $i = 3$ and $R = 4r_0 = 2d_0 = 2 \times 1.2 = 1.4$ mm. From Eq. (5-84) it follows that

$$d_p = \sqrt{\frac{2Rd_0}{iK}} = \sqrt{\frac{2 \times 2.4 \times 1.2}{3 \times 0.9}} = 1.46 \text{ mm}$$

The Reynolds number from Eq. (5-86) equals

$$\mathrm{Re} = \frac{4G}{\pi\rho\nu\sqrt{i}\,d_p} = \frac{4 \times 0.04}{\pi \times 830 \times 2.2 \times 10^{-6}\sqrt{3} \times 1.46 \times 10^{-3}}$$
$$= 11{,}080$$

From Eq. (5-87) we obtain

$$\lg\lambda = \frac{25.8}{(\lg \mathrm{Re})^{2.58}} - 2 = \frac{25.8}{(\lg 11\,080)^{2.58}} - 2 = -1.3$$

Therefore

$$\lambda \approx 0.051$$

After substitution, we obtain from Eq. (5-81)

$$K_\lambda = \frac{Rr_0}{ir_p^2 + (\lambda/2)R(R - r_0)} = \frac{2.4 \times 0.6}{3 \times 0.73^2 + (0.051/2)2.4(2.4 - 0.6)}$$
$$= 0.843$$

As seen, constant K_λ differs only slightly from constant K and therefore the viscosity effect can be neglected.

Independently, assuming 5% accuracy, i.e., assuming the ratio of flow ratios $\Phi = 1.05$, we obtain from inequality (5-88)

$$\frac{2}{\lambda}(\Phi^{1.5} - 1) = \frac{2}{0.051}(1.05^{1.5} - 1) = 2.9$$

and

$$\frac{B^2}{i} - K = \frac{(2.4/0.73)^2}{3} - 0.9 = 2.7 < 2.9$$

which also indicates that viscosity can be neglected.

Assuming counteraction coefficient $\varphi = 0.9$, we obtain from Eq. (5-89) the corrected diameter of the inlet orifice d_p'

$$d_p' = \frac{d_p}{\sqrt{\varphi}} = \frac{1.46}{\sqrt{0.9}} \approx 1.55 \text{ mm}$$

The remaining dimensions of the atomizer are

$D_s = 2R + d_p' = 2 \times 2.4 + 1.55 = 6.35$ mm
$l_s = 2$ mm $> d_p'$
$l_p = 2 \times d_p' = 2 \times 1.55 = 3.1$ mm
$l = 0.5d_0 = 0.5 \times 1.2 = 0.6$ mm
$\beta = 90°$

5-2.2 Duplex Atomizers

Duplex atomizers. The design of duplex atomizers is a complex one, since jets interact in a common swirl chamber [15]. The most complex state of flow exists when the control valve is partially open (Fig. 4-27). The Bernoulli equation has the following form.

For primary feeding:

$$P_t = P_{p1} + \frac{\rho v_{p1}^2}{2}(1 + \zeta_1) \tag{5-90}$$

For secondary feeding:

$$P_t = P_{p2} + \frac{\rho v_{p2}^2}{2}(1 + \zeta_2) \tag{5-91}$$

where ζ_1, ζ_2 are the coefficients of local losses in the inlet channels. ζ_1 = const for primary feeding. For secondary feeding coefficient ζ_2 varies from $\zeta_2 = \infty$ for the closed valve to $\zeta_2 = 0$ when the control valve is open. Since in the common swirl chamber $P_{p1} = P_{p2} = P_p$, it follows from Eqs. (5-90) and (5-91) that

$$v_{p2} = v_{p1}\sqrt{\frac{1 + \zeta_1}{1 + \zeta_2}} \tag{5-92}$$

The equation of conservation of angular momentum in the swirl chamber has the following form:

$$Gv_pR = G_1v_{p1}R + G_2v_{p2}R$$

where G, G_1, G_2 are the mass flow rates and, v_p is the resultant velocity on the radius R.

From the equation of conservation of angular momentum it follows that

$$v_p = \frac{G_1v_{p1} + G_2v_{p2}}{G} \tag{5-93}$$

The equation of flow continuity has the following form:

$$G = G_1 + G_2 = \pi\rho\left(i_1r_{p1}^2v_{p1} + i_2r_{p2}^2v_{p2}\right) \tag{5-94}$$

Substituting Eq. (5-92), we obtain

$$G = \pi\rho\bar{r}_p^2\bar{v}_{p1} \tag{5-95}$$

where

$$\bar{r}_p = \sqrt{i_1 r_{p1}^2 \left(1 + \kappa \sqrt{\frac{1+\zeta_1}{1+\zeta_2}}\right)} \tag{5-96}$$

$$\kappa = \frac{i_2 r_{p2}^2}{i_1 r_{p1}^2} \tag{5-97}$$

Equation (5-93), after accounting for Eqs. (5-94) and (5-92), assumes the form

$$v_p = v_{p1} \frac{1 + \kappa(1+\zeta_1)/(1+\zeta_2)}{1 + \kappa\sqrt{(1+\zeta_1)/(1+\zeta_2)}} \tag{5-98}$$

Denoting

$$\bar{R} = R \frac{1 + \kappa(1+\zeta_1)/(1+\zeta_2)}{1 + \kappa\sqrt{(1+\zeta_1)/(1+\zeta_2)}} \tag{5-99}$$

then the angular momentum for a unit volume of the liquid equals

$$M = \rho v_p R = \rho v_{p1} \bar{R} \tag{5-100}$$

By the same reasoning as for a simplex atomizer, and using Eqs. (5-95) and (5-100), we arrive at the conclusion that for a duplex atomizer the role of geometric constant K is played by constant $\bar{K}$:

$$\bar{K} = \frac{\bar{R} r_0}{\bar{r}_p^2} \tag{5-101}$$

Discharge coefficient μ and spray angle α of a duplex atomizer can be determined from Fig. 5-11, if constant K is replaced by constant $\bar{K}$. Substituting $\bar{r}_p$ from Eq. (5-96) and $\bar{R}$ from Eq. (5-99) in Eq. (5-101), we obtain

$$\bar{K} = \sigma K_1 \tag{5-102}$$

where

$$\sigma = \frac{1 + \kappa(1+\zeta_1)/(1+\zeta_2)}{\left(1 + \kappa\sqrt{(1+\zeta_1)/(1+\zeta_2)}\right)^2} \tag{5-103}$$

and geometric constant K_1 is expressed by Eq. (4-4). From Eq. (5-102) it follows that when the control valve is closed ($\zeta_2 = \infty$), $\bar{K} = K_1$, and when the valve is completely open ($\zeta_2 = 0$), constant $\bar{K}$ is close to constant K_2 and for $\zeta_1 = 0$, $\bar{K} = K_2$. Geometric constant K_2 is expressed by Eq. (4-5). Constant $\bar{K}$ therefore falls in the range $K_2 \leq K < K_1$.

Knowing flow rate G, we can determine flow rate G_1 of the first and G_2 of the second feed system. Implementing Eqs. (5-92), (5-93), (5-94), and (5-98), we

obtain

$$G_1 = \frac{1}{1 + \kappa\sqrt{(1 + \zeta_1)/(1 + \zeta_2)}} G \tag{5-104}$$

$$G_2 = \frac{\kappa\sqrt{(1 + \zeta_1)/(1 + \zeta_2)}}{1 + \kappa\sqrt{(1 + \zeta_1)/(1 + \zeta_2)}} G \tag{5-105}$$

Here the energy loss in the control valve and losses of mixing of the first and second feed jets in the swirl chamber were omitted. These losses in the range $\kappa = 4-10$ do not exceed 15–20% of the total energy of the liquid, so they can be neglected in technical calculations.

Duplex atomizers are used for small liquid viscosities. When it is necessary to take the viscosity into account, the approach is as follows. From Eqs. (5-95), (5-100), and (5-102) it follows that the equivalent geometric constant for a partially open control valve is

$$K_\lambda = \frac{\sigma K_1}{1 + (\lambda/2)\sigma(B_1^2/i_1 + K_1)} \tag{5-106}$$

where $B_1 = R/r_{p1}$.

The Reynolds number equals

$$\mathrm{Re} = \frac{v_p d_p}{\nu}$$

Velocity v_p can be calculated from Eq. (5-98). To do so, we substitute

$$v_{p1} = \frac{4G_1}{\rho i_1 \pi d_{p1}^2}$$

and G_1 from Eq. (5-104) and σ from Eq. (5-103). As a result we obtain

$$v_p = \frac{4\sigma G}{\pi i_1 \rho d_{p1}^2}$$

Diameter d_p equals

$$d_p = \frac{i_1 d_{p1} + i_2 d_{p2}}{i_1 + i_2}$$

After substituting,

$$\mathrm{Re} = \frac{4\sigma G(i_1 d_{p1} + i_2 d_{p2})}{\pi i_1 \rho d_{p1}^2 \nu (i_1 + i_2)} \tag{5-107}$$

Using Eq. (5-107), we calculate friction coefficient λ from formula (5-87). With Eq. (5-106), it is possible to determine geometric constant K_λ.

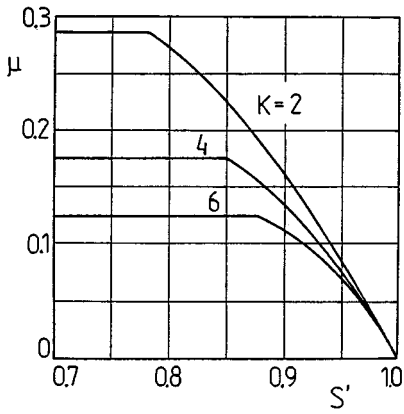

Figure 5-14 Relationship $\mu = f(K, S')$ for the secondary feeding system of a duplex atomizer.

Two-nozzle atomizers. In two-nozzle atomizers, liquid flow through both systems proceeds independently (Fig. 4-31), which significantly simplifies the calculations [15]. The design of a two-nozzle atomizer consists of separate calculations for two systems following the method described for simplex atomizers. The relative position of the two nozzles (discharge orifices) affects the shape of the spray, which will be discussed further in Sec. 6-2. The first feeding system of a two-nozzle atomizer operates at low liquid flow rates, which leads to small Reynolds numbers and high values of $(B^2/i - K)$ due to the small diameter of the inlet orifices. In this situation the calculations for the first feeding system take into account viscosity effects.

During calculations one should pay attention to the diameter of the gas core of the secondary flow system. If the core diameter is larger than the outer diameter of the nozzle of the first system, the design of the secondary system proceeds exactly as for a simplex atomizer. However, if the core diameter is smaller (which leads to disturbances during the flow through the second stage), one should use Eq. (5-58), assume $S = S' = r'/r_0$, where r' denotes the outer diameter of the nozzle of the first stage.

Solving Eq. (5-58) graphically, we obtain the function $\mu = f(K, S')$. The solution is shown in Fig. 5-14. As seen, discharge coefficient μ of the secondary stage of the atomizer starts to decrease rapidly when S' exceeds a certain value. These results have been confirmed experimentally.

5-2.3 Spill-Return Atomizers

This design will concern spill-return atomizers operating in the one-way system regime (Fig. 4-34) [15]. The reasoning will be limited to the case of an ideal liquid.

The flow rate of the liquid discharging through the outlet orifice is

$$G_a = \mu \pi r_0^2 \sqrt{2 \rho P_t} \tag{5-108}$$

Flow rate μ during the return of the liquid is a function not only of geometric constant K but also of the flow rate of the returned liquid G_d, and according to Eq. (4-7) the total flow rate equals

$$G_t = G_a + G_d$$

The geometric constant assumes the form

$$K = \frac{Rr_0}{ir_p^2}$$

Flow rate G_d can be expressed in the same way as in Eq. (5-59), namely

$$G_a = \epsilon\rho\pi r_0^2 u \tag{5-109}$$

Axial component u can be expressed by using Eq. (5-55):

$$u = \sqrt{\frac{2P_t}{\rho} - v_{\max}^2} \tag{5-110}$$

According to Eq. (4-8), the excess liquid coefficient is

$$e = \frac{G_t}{G_a} = 1 + \frac{G_d}{G_a}$$

The total flow rate of the liquid, using Eq. (5-108), is

$$G_t = eG_a = e\mu\pi r_0^2\sqrt{2\rho P_t} \tag{5-111}$$

When there is no liquid return ($G_d = 0$), the excess liquid coefficient equals $e = 1$ and Eq. (5-111) transforms to Eq. (5-108), i.e., $G_t = G_d$.

Now we should use Eq. (5-49)

$$v_{\max} r_r = v_p R \tag{5-112}$$

Velocity v_p at the inlet to the swirl chamber can be expressed as in Eq. (5-60), namely

$$v_p = \frac{G_t}{\rho i\pi r_p^2} \tag{5-113}$$

From Eqs. (5-111) to (5-113) we obtain

$$v_{\max} = \frac{e\mu R r_0^2}{ir_r r_p^2}\sqrt{\frac{2P_t}{\rho}} \tag{5-114}$$

Equation (5-109), after substitution of Eqs. (5-45), (5-109), (5-110), and (5-114) into it, assumes the following form:

$$G_a = \epsilon\pi r_0^2\sqrt{\left(1 - \frac{\mu^2 e^2 K^2}{1-\epsilon}\right)2\rho P_t} \tag{5-115}$$

Comparing Eqs. (5-108) and (5-115), we obtain the value of the flow ratio

$$\mu = \epsilon\sqrt{1 - \frac{\mu^2 e^2 K^2}{1 - \epsilon}}$$

and after further transformation

$$\mu = \frac{1}{\sqrt{K_d^2/(1 - \epsilon) + 1/\epsilon^2}} \tag{5-116}$$

As seen, Eq. (5-116) differs from Eq. (5-64) in that, instead of geometric constant K, constant K_d appears. K_d is expressed by Eq. (4-9). The relationship between the filling efficiency ϵ and the geometric constant of a spill-return atomizer K_d can be determined on the basis of the principle of the maximum flow. According to this principle, condition $d\mu/d\epsilon = 0$ should be satisfied. Excess liquid coefficient e is a function of ϵ, but in the range of the maximum flow it is almost constant. In this situation the dependence of discharge coefficient μ on geometric constant K_d has the same character as the dependence of μ on K for a simplex atomizer. The same refers to angle α. As coefficient e increases, coefficient μ decreases and angle α increases.

5-2.4 Variable-Geometry Atomizers

The control of the area of the tangential inlet orifices to the swirl chamber causes the geometric constant of the atomizer to change. During the uncovering of the orifices the geometric constant decreases from K_1 to K_2, where

$$K_1 = \frac{Rr_0}{i_1 r_p^2}, \qquad K_2 = \frac{Rr_0}{i_2 r_p^2}$$

where i_1, i_2 are the numbers of uncovered orifices for the initial and final positions of the needle, respectively. It was assumed in this case that the inlet orifices are identical. In the range K_1 to K_2 the values of the discharge coefficient μ and the angle α must be determined from Fig. 5-11.

The needle is acted on by the pressure and spring forces. Using the equations of flow continuity, conservation of momentum, and angular momentum results in the following equation, which expresses the pressure (overpressure) distribution in the swirl chamber:

$$P = P_t\left[1 - \frac{\mu^2 r_0^4}{i_1 r_p^2}\left(\frac{1}{16} + \frac{R^2}{r_p^2}\right)\frac{1}{r^2}\right] \tag{5-117}$$

Assuming $P = 0$, we can determine the radius of the gas core in the swirl chamber, r_r'' (Fig. 5-9):

$$r_r'' = \mu r_0 K\sqrt{1 + \frac{r_p^2}{16R^2}} \tag{5-118}$$

The expression under the square root is close to unity, hence Eq. (5-118) assumes the form

$$\frac{r_r''}{r_0} = \mu K \tag{5-119}$$

Function $r_r''/r_0 = f(k)$ is shown in Fig. 5-10.

Equation (5-117) therefore assumes the form

$$P = P_t\left(1 - \frac{r_r''^2}{r^2}\right) \tag{5-120}$$

Radius r varies in the range $r_r'' \leq r \leq R_s$, where R_s is the radius of the swirl chamber. Determining the pressure distribution makes it possible to calculate the force acting on the needle spring:

$$F = \int_{r_r''}^{R_s} P 2\pi r\, dr$$

Substituting P from Eq. (5-120) and integrating yield

$$F = 2\pi P_t\left[\frac{1}{2}\left(R_s^2 - r_r''^2\right) - r_r''^2 \ln\frac{R_s}{r_r''}\right] \tag{5-121}$$

In order to take into account viscosity, one should use not constant K but equivalent constant K_λ from Eq. (5-77). The viscosity effect is especially visible for low pressures P_t when only some orifices are uncovered.

5-3 DESIGN OF JET-SWIRL ATOMIZERS

5-3.1 Ideal Liquid Theory [16, 17]

In a swirl chamber and especially in the discharge orifice, an interaction occurs between the unswirled (axial) and swirled jets (Fig. 5-15). The *unswirled jet* flows with axial velocity u_a. The *swirled jet* moves along the walls of the swirl chamber with a resultant velocity in which the dominant role is played by the circumferential components of velocity. Both jets enter the discharge orifice, where the swirled jet has circumferential component v and axial component $u < u_a$.

In the discharge orifice on the boundary between two jets a *turbulent boundary layer* develops in which significant shear stresses exist. As a result, equalization of the axial components of both jets occurs and a certain circumferential velocity is set for the unswirled jet. The turbulent processes cause not only energy exchange but also mass exchange. A theoretical solution does not exist for these processes, so empirical-theoretical solutions are used.

The following assumptions will be made:

1. Liquid motion inside the atomizer has a turbulent character, and therefore the velocity distributions are approximately uniform.